Organic Electronics 13 (2012) 604–614

Contents lists available at SciVerse ScienceDirect

Organic Electronics

journal homepage: www.elsevier.com/locate/orgel

Synthesis and characterization of porphyrin electrochromic and photovoltaic electropolymers

Javier Durantini [a], Gustavo M. Morales [a], Marisa Santo [b], Matías Funes [a], Edgardo N. Durantini [a], Fernando Fungo [a], Thomas Dittrich [c], Luis Otero [a,*], Miguel Gervaldo [a,*]

[a] Departamento de Química, Universidad Nacional de Río Cuarto, Agencia Postal Nro. 3, X5804BYA Río Cuarto, Córdoba, Argentina
[b] Departamento de Física, Universidad Nacional de Río Cuarto, Agencia Postal Nro. 3, X5804BYA Río Cuarto, Córdoba, Argentina
[c] Helmholtz Center Berlin for Materials and Energy, Institute of Heterogeneous Materials, Hahn-Meitner-Platz 1, D-14109 Berlin, Germany

ARTICLE INFO

Article history:
Received 20 September 2011
Received in revised form 2 December 2011
Accepted 5 January 2012
Available online 17 January 2012

Keywords:
Porphyrin
Carbazole
Triphenylamine
Electropolymerization
Electrochromic
Surface photovoltage

ABSTRACT

New asymmetric porphyrins, with electroactive functionalities were synthesized. 5,15-Bis[4(-*N*,*N*-diphenylamino)phenyl]-10,20-bis[3-(*N*-ethylcarbazoyl)]porphyrin and its Zn(II) derivative allow the electrochemical formation of conjugated, conducting and stable polymeric films over semitransparent indium–tin oxide surface. The spectral changes observed upon oxidation of the films produced different colorations. The polymeric materials showed the generation of photoinduced charge separation states and charge migration upon porphyrin excitation, making them promising candidates for application in optoelectronics devices.

1. Introduction

In the development of optoelectronic devices, organic molecular compounds are receiving great attention as promising constituents due to their advantages over conventional semiconductor electronics. Molecular engineering (often assisted by computational methods [1,2]) and the development of synthesis routes allow the generation of organic compounds with the desired physical properties for application as building blocks of optoelectronic devices. In this context it deserves special consideration the use of organic conducting polymers [3–6]. It is reasonable to expect that the development of organic polymers with adequate optical and electronic properties will introduce a significant advance in the construction and application of devices for energy generation, image display, lighting systems and others. However, the use of organic polymers in electronics faces the difficulty of polymer film deposition over conducting or semiconducting contact. Up to now, two major approaches are used to deposit organic material thin films in optoelectronic devices: thermal evaporation and solution-processing. Thermal evaporation requires materials with high sublimation capability and excellent thermal stability, which are properties not easily obtained in polymers. On the other hand, low-cost solution processes, such as spin-coating and deep-coating, widely used in the production of non-patterned films, require materials with intrinsic high solubility, and usually produce large amounts of waste. An alternative technique to produce promising conducting polymer films is the electropolymerization, with the adoption of electroactive monomers. The polymerization through electrochemical deposition techniques allows synthesizing the polymeric film in one step with fine control over the thickness; moreover, a mold in the working electrode allows an excellent and simple pattern of the film. A number of reports revealed that the polymeric films obtained electrochemically over conductive solid substrates

* Corresponding authors.
E-mail address: mgervaldo@exa.unrc.edu.ar (M. Gervaldo).

1566-1199/$ - see front matter © 2012 Elsevier B.V. All rights reserved.
doi:10.1016/j.orgel.2012.01.004

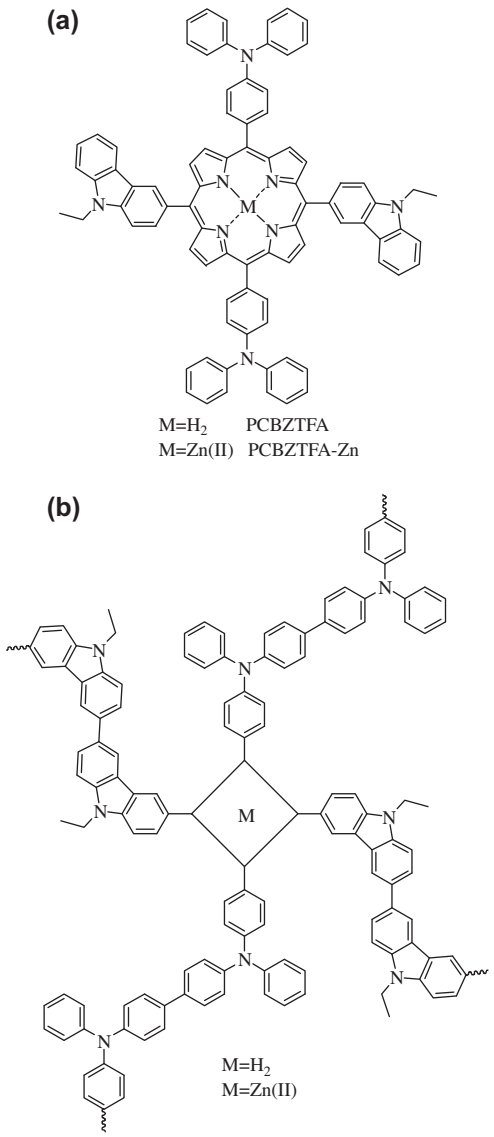

Fig. 1. Chemical structure of the monomers (a) and idealized polymer structure (b).

are highly stable, showing compact layers, with excellent stuck to the electrode and high charge transport capability [7–15].

A considerable number of organic structures has been designed, synthesized and studied with the purpose of being used as precursors of organic electropolymers in the development of optoelectronic devices. In this frame, many researchers inspired by the natural photosynthetic apparatus incorporated porphyrins, chlorophyll derivatives, and several related metallized and unmetallized tetrapyrrolic compounds in the development of organic photovoltaic devices [16–21]. Porphyrins accept or donate electrons easily through their large π electron frameworks, they are suitable for electronic conduction, and together with their optical properties, porphyrins become in one of most useful structures in organic optoelectronic devices. There are several examples of generation of porphyrin polymers by electrochemical [20,22,23] or chemical [16,19,24–26] methods and their use as components in electronic or optoelectronic devices. Even more, a *p*/*n* heterojunction device where the donor and acceptor layers were electrochemically deposited has recently been reported [27].

In this work we show the monomers synthesis, polymers electrosynthesis, spectroelectrochemical characterization and surface photovoltage spectroscopy of novels 5,15-bis[4(-*N*,*N*-diphenylamino)phenyl)]-10,20-bis[3-(*N*-ethylcarbazoyl)]porphyrin (PCBZTPA) and Zn(II) 5,15-bis[4(-*N*,*N*-diphenylamino)phenyl)]-10,20-bis[3-(*N*-ethylcarbazoyl)]porphyrin (PCBZTPA-Zn, Fig. 1) conducting polymer films. Upon oxidation, both carbazol (CBZ) and triphenylamine (TPA) moieties undergo the well-known radical cation dimerizations [7,12,37,47] producing dicarbazol (DCBZ) and tetraphenylbenzidine (TPB) units, which conduct to porphyrin electropolymer formation [7,12]. However, in general, the CBZ radical cation has coupling rate constants that are 4–5 orders of magnitude higher than those of the TPA groups [28], and as a consequence we expected that CBZ dimerization moieties led to the formation of a linear polymer due to the cross positions of the CBZ residues in the monomer structure, meanwhile TPA dimerizations allow a polymer cross-linkage during the electropolymerization. CBZ dimers and polymers usually exhibit high electrical conductivity and good optical quality, giving them great potential for use in optoelectronic applications [29–33]. The films formed over conducting indium tin oxide semitransparent electrodes showed the generation of photoinduced charge separation states. This fact indicates that electropolymerized films of PCBZTPA and PCBZTPA-Zn could be promising in a variety of applications, for example for the construction of polymeric organic solar cells, since they are strong visible light absorbers and good electronic conductors.

2. Experimental

2.1. PCBZTPA and PCBZTPA-Zn synthetic procedure

PCBZTPA was synthesized from *meso*-[4-(*N*,*N*-diphenylaminophenyl)]dipyrromethane. Thus, a solution of 4-(*N*,*N*-diphenylamino)benzaldehyde (1.96 g, 7.17 mmol) and pyrrole (24 mL, 346 mmol) was purged in an argon atmosphere for 15 min at room temperature. The reactions were initiated by addition of trifluoroacetic acid (TFA, 138 μL, 1.79 mmol) and stirred for 30 min under the same conditions. The reaction was terminated by addition of triethylamine (TEA, 760 μL, 5.46 mmol) and diluted with 50 mL of dichloromethane (DCM). Finally, volatile compounds were removed under reduced pressure, and the unreacted pyrrole was removed by vacuum distillation at 60 °C. The product obtained was purified by flash column chromatography (silica gel, cyclohexane/ethyl acetate/TEA 80:20:1), yielding 1.96 g (70%) of pure dipirrometane. TLC (silica gel, cyclohexane/ethyl acetate/TEA 80: 20:1) R_f = 0.25. ^{1}H NMR ($CDCl_3$, TMS) δ [ppm] 5.43 (s, 1H, *meso*-H); 5.94 (m, 2H, pyrrole-H); 6.17(q, 2H, pyrrole-H);

6.72 (m, 2H, pyrrole-H); 6.94–7,12 (m, 10 H, –ArH); 7.22 (m, 4 H, –ArH); 7.98 (s, brs, 2H, pyrrole NH). ESI-MS [m/z] 389.1892 (M^+). A solution of *N*-ethyl-3-carbazolecarbaldehyde (0.56 g, 2.50 mmol) and dipyrromethane (1.00 g, 2.50 mmol) in 310 mL of DCM was purged with argon for 15 min. After that, trifluoroacetic acid (425 μL, 5.50 mmol) was slowly added and the solution was stirred for 60 min at room temperature. Then, 2,3-dichloro-5,6-dicyano-1,4-benzoquinone (DDQ, 1.50 g, 6.61 mmol) was added and the mixture was stirred for an additional 18 h, open to the atmosphere. The solvent was removed under reduced pressure. The obtained product was purified by flash column chromatography (silica gel, hexane/DCM/TEA 6:93.8:0.2) obtaining 622 mg (42%) of pure PCBZTPA. TLC (silica gel, hexane/DCM/TEA 6:93.8:0.2) R_f = 0.68. ^{1}H NMR ($CDCl_3$, TMS) (ppm) δ −2.60 (brs, 2H, pirrol N–H); 1.68 (t, 6H, $-CH_3$, J = 7.1 Hz); 4.64 (q, 4H, $-CH_2-$, J = 7.1 Hz); 7.15 (d, 4H, J = 7.8 Hz); 7.34–7.50 (m, 22 H); 7.52–7.64 (m, 4 H); 7.75 (d, 2H, J = 8.3 Hz); 8.02 (d, 4H, J = 7.8 Hz); 8.20 (d, 4 H, J = 7.7 Hz), 8.34 (d, 2H, J = 8.3 Hz), 8.82–9.06 (d, 8H). ESI-MS [m/z] 1183.5176 $[M+H]^+$ (1182.5097 calculated for $C_{84}H_{62}N_8$). PCBZTPA-Zn was obtained from PCBZTPA. A solution of PCBZTPA (40 mg, 0.034 mmol) in 8 ml of DCM was treated with 3 mL of a saturated solution of zinc(II) acetate in methanol. The mixture was stirred for 1 h in argon atmosphere at room temperature. After that, the solution was treated with water (30 mL) and the organic phase was extracted with three portions of DCM (20 mL each). The solvents were evaporated under reduced pressure. The reaction afforded 41 mg (97%) of pure PCBZTPA-Zn. ESI-MS [m/z] 1245.4311 $[M+H]^+$ (1244.4232 calculated for $C_{84}H_{60}N_8Zn$).

2.2. Instrumentation and measurements

The spectroscopic (absorption–emission), electrochemical and spectroelectrochemical characterization of the new organic materials was performed using the already described set-up [7–12] Electrochemical studies were carried out over Pt and indium tin oxide (ITO) electrodes (Delta Technologies nominal resistance of 8–12 Ω/square) in 1,2-dichloroethane (DCE) deoxygenated solution (nitrogen bubbling), with 0.10 M tetra-*n*-butylammonium hexafluorophosphate ($TBAPF_6$) as the supporting electrolyte. A silver wire quasi-reference electrode was used. The Pt working electrode was cleaned between experiments by polishing with 0.3 μm alumina paste followed by solvent rinses. After each voltammetric experiment, ferrocene was added as an internal standard, and the potential axis was calibrated against the formal potential for the Saturated Calomel Electrode (SCE).

The measurements of modulated Surface Photovoltage (SPV) were performed in the fixed capacitor arrangement with chopped light (modulation frequency 6 Hz) from a quartz prism monochromator (SPM2) and a halogen lamp (100 W). The measurements were carried out in vacuum using an already described set-up [34]. SPV transients were excited with laser pulses (wavelength 600 nm, time of laser pulses: 5 ns, intensity: about 3 mJ/cm^2) and recorded with a sampling oscilloscope (GAGE compuscope CS 14200) at resolution of 10 ns. The intensity of exciting light was changed with calibrated neutral density filters over several orders of magnitude [34].

Atomic force microscopy (AFM) experiments were performed using an Agilent 5500 SPM microscope (Agilent Technologies, Inc.) working in Acoustic AC Mode. Commercial silicon cantilever probes, with aluminum backside coating, and nominal tip radius of 10 nm (MikroMasch, NSC15/Al BS/15, spring constant ranging 20–75 N m^{-1}), were employed just under their fundamental resonance frequencies of about 325 kHz.

The thickness of the polymer films were also measured with a surface profiler (Dektak 8 Advanced Development Profiler system, Veeco).

3. Results and discussion

3.1. Absorption and emission properties

The absorption spectra of the porphyrins in DCM solution and of the films on ITO electrodes are shown in Fig. 2a. The PCBZTPA and PCBZTPA-Zn porphyrins show the typical *Soret* and *Q*-bands, characteristic of a free-base porphyrin and the corresponding Zn(II) metalloporphyrin [35]. Also, the porphyrins in solution show an absorption band in the UV region (∼305 nm) due to the CBZ and TPA substituents. The steady-state fluorescence emission spectrum of the porphyrins in DCM are shown in Fig. 2b. The two bands are characteristic of free-base and Zn-substitued porphyrins in solution, being these assigned to *Q*(0–0) and *Q*(0–1) transitions [36].

3.2. Electrochemical characterization

The electrochemical properties of PCBZTPA and PCBZTPA-Zn monomers were investigated by cyclic voltammetry in DCE containing $TBAPF_6$ using a Pt working electrode. Fig. 3a and b show the first anodic and cathodic scan of the monomers. In order to obtain more detailed information about the electrochemical processes CVs were recorded at different inversion potentials. PCBZTPA shows two reduction peaks and three oxidation processes whereas PCBZTPA-Zn shows one reduction peak and four oxidation processes. In the anodic scan the first oxidation peak detected for PCBZTPA and the first two for PCBZTPA-Zn are attributed to porphyrin macrocycle oxidation. The difference observed in the number of peaks could be attributed to substitution of the two H central atoms in PCBZTPA by Zn(II), which lowers the first oxidation potential in PCBZTPA-Zn and as a result two peaks are observed. The two remaining oxidation peaks of PCBZTPA detected at more anodic potentials may be attributed to oxidation of the TPA and CBZ groups attached to the porphyrin macrocycle being the CBZ groups oxidized at more anodic potentials than TPA [28,37]. For PCBZTPA-Zn a similar assignment could be made with the difference that these two last peaks occur at less anodic applied potentials than PCBZTPA, due to the presence of the Zn(II) central metal.

Continuous cycling of the monomers through the furthest oxidation peak produces an increase in the intensity of the oxidation and reduction currents and clearly new

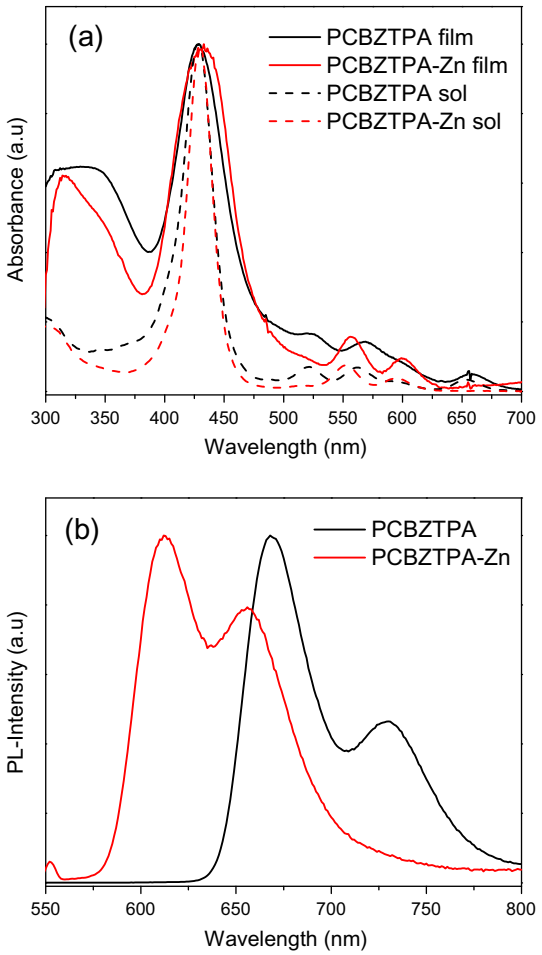

Fig. 2. (a) Electronic absorption spectra of PCBZTPA (solid black) and PCBZTPA-Zn (solid red) in DCM solution, and PCBZTPA film (dashed black) and PCBZTPA-Zn film (dashed red) on ITO. (b) Fluorescence spectra of PCBZTPA and PCBZTPA-Zn in DCM solution. (For interpretation of the references to color in this figure legend, the reader is referred to the web version of this article.)

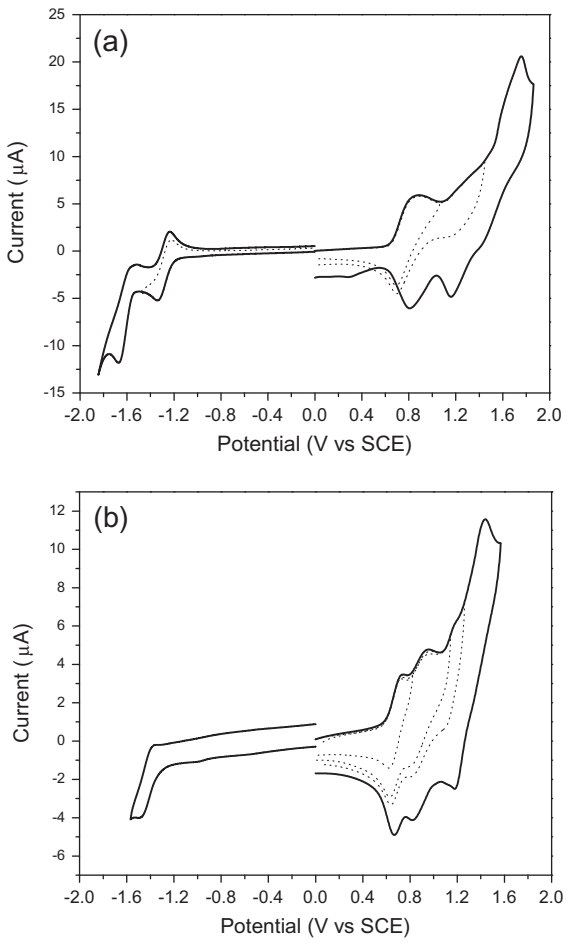

Fig. 3. Cyclic voltammetry (at different inversion potentials) of PCBZTPA (a) and, PCBZTPA-Zn (b) in DCE solution containing 0.1 M $TBAPF_6$. Platinum working electrode, scan rate: 100 mV/s.

redox systems can be detected, indicating the formation of electroactive films on the working electrode surfaces (Fig. 4a and b). To confirm the absorption of the films on the electrode their electrochemical response were recorded in monomer-free electrolytic solution (Fig. 5a and b). Two reversible redox couples are detected for PCBZTPA and they appear at around 0.83 and 1.17 V. PCBZTPA-Zn also shows two redox couples which occur at oxidation potential values similar to those observed for PCBZTPA. Also the oxidation/reduction peak currents for both films increase linearly with the scan rate which is indicative of an electro-active product irreversibly adsorbed on the electrode. On the other hand, if the monomers are repetitively scanned through the peaks assigned to oxidation of the triphenylamine (TPA) units, an increase in the oxidation/reduction current peaks is also detected, but this is smaller than that observed when the furthest oxidation peak was cycled. When the electrodes were removed from the monomer solutions and placed in a solution containing only support electrolyte both films showed two redox couples. The oxidation potentials of the films were similar to the ones observed when the films were grown cycling the most anodic oxidation peak, but the magnitudes of the oxidation/reduction currents were smaller. This indicates that the polymerization efficiency is lower when the film is grown cycling the peak assigned to oxidation of the TPA groups. No increase in the oxidation/reduction currents was detected when the peaks assigned to porphyrin oxidation were continuously cycled.

Previous electrochemical results in porphyrins have shown that substitution of the two hydrogen central atoms by metals alters the reduction and oxidation processes [38,39]. For example, substitution by Pd(II) increases the oxidation potential by 160 mV whereas substitution by Zn(II) decreases the oxidation potential [40]. Substitution at the meso position of the macrocycle also modifies the redox properties. We observed in a related porphyrin substituted with TPA groups two oxidations peaks, being the first one attributed to oxidation of the macrocycle (2 electron processes) and the second one to oxidation of the TPA units [7]. Contrarily, substitution by four carbazole

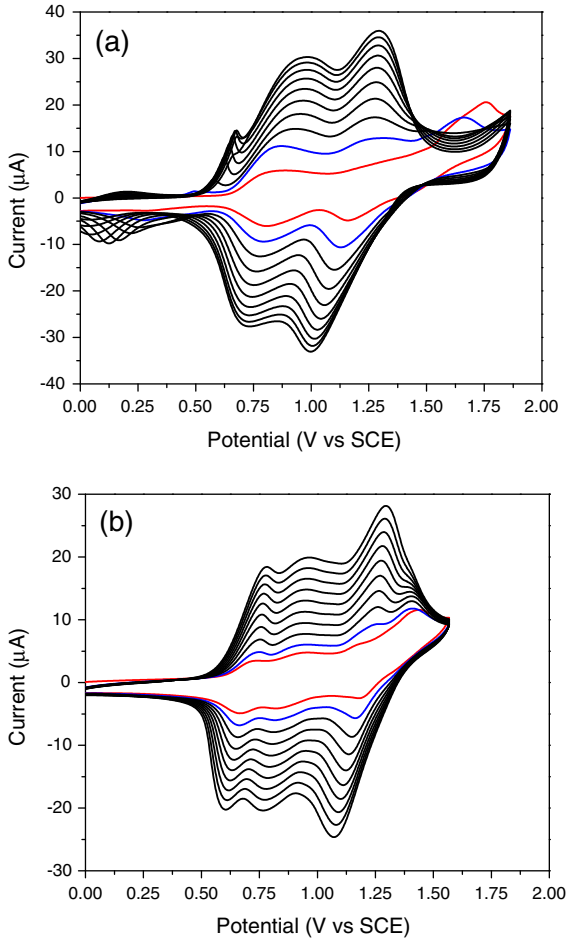

Fig. 4. Cyclic voltammograms of PCBZTPA (a) and PCBZTPA-Zn (b), showing repetitive anodic sweeps at a platinum electrode immersed in a solution of monomer as described in Fig. 2. A total of 10 scans are shown.

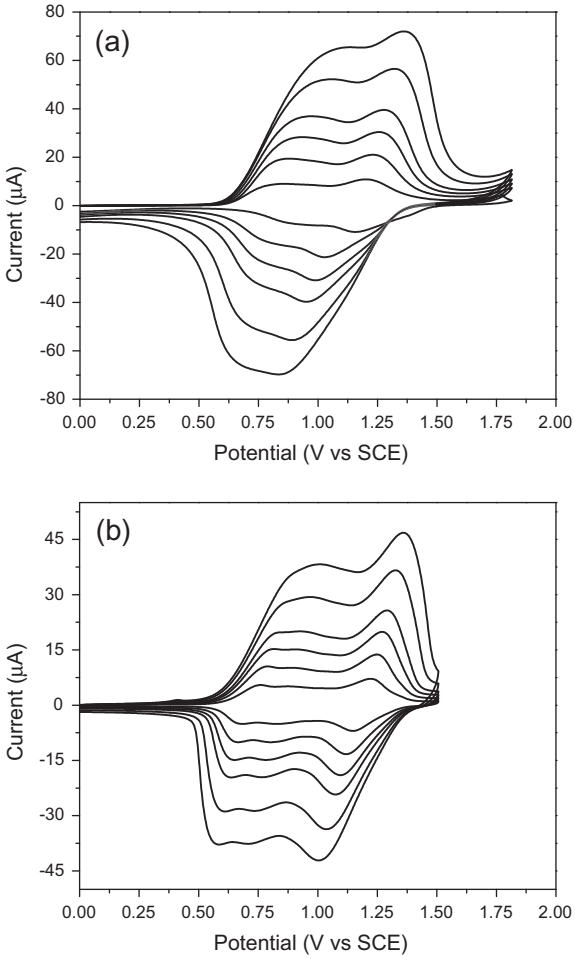

Fig. 5. Cyclic voltammograms of electropolymerized films of PCBZTPA (a) and PCBZTPA-Zn (b) resulting from Fig. 3. Scan rates: 200, 150, 100, 75, 50, 25 mV/s.

(CBZ) groups showed three oxidations, which were assigned to formation of porphyrin radical cation and dication, and to oxidation of the CBZ groups, respectively [12]. On the other hand, in general CBZ and TPA present a similar electrochemistry [41–44]. Oxidation of any of both monomers, CBZ or TPA, leads to formation of highly reactive radical cations, which then couple with other radical cations to form dimers, being these dimers more easily oxidized than the monomers. Moreover, related CBZ and TPA based polymers have shown two oxidation processes, which have been assigned to radical cation and dication of dicarbazole (DCBZ) and tetraphenylbenzidine (TPB), respectively [45–48]. Comparison of coupling rate constants has shown that CBZ has a 4–5 order of magnitude higher constant than those of TPA groups [28]. It must be remarked that in PCBZTPA and PCBZTPA-Zn the CBZ and TPA units are conjugated with the porphyrin macrocycle. Therefore, it is highly possible that the monomers do not behave as a porphyrin formed by three independent units i.e. porphyrin macrocycle, two CBZ and two TPA units, but like a whole molecule with all these groups connected and interacting. This "connection" between the different units could affect the electrochemical properties. Oxidation of the porphyrin may lead to charge delocalized not only over the macroclycle, also over the CBZ and TPA groups. In the same way the third electron could be removed from the TPA, but the resulting positive charge may also delocalize over the whole molecule.

3.3. Spectroelectrochemical characterization

Spectroelectrochemistry of the films was done in order to gain more information about the oxidation processes and to clarify the polymerization mechanism. When the films are in the neutral state the spectra show the characteristic porphyrin Soret bands and also the four and two Q typical bands of free base and Zn(II) derivative, respectively (Fig. 2a). These bands are quite similar to those observed for the monomer in solution, indicating that the macrocycles have not been altered during the polymerization processes, although the bands of PCBZTPA film and PCBZTPA-Zn film are broader and shifted in comparison

with those of monomeric porphyrins in solution. These facts indicate the presence of interaction between porphyrins in the branched film structure. Fig. 6a and b show absorption spectra of the films (plotted as ΔAbs) at different applied potentials when the films were grown cycling: (1) the peak assigned to oxidation of TPA units and (2) the peak assigned to oxidation of CBZ units. During oxidation two bands develop for both films in (1). For the free base the first one is located at about 485 nm and the second band appears as broad band between 500 and 1000 nm with a maxima at around 710 nm. For the Zn derivative the first band appears at 510 nm, and the broad band has a maximum at 720 nm. The bands at 485–510 nm start growing at the onset potential of the first oxidation peaks for both films, and then decrease at more anodic potentials. At the beginning of the second oxidation peaks the broad bands (maximum 710–720 nm) increase, and they reach the highest absorption when the films are completely oxidized. During the entire oxidation process the bleaching of the Soret bands increases in intensity together with a small change in the bands detected in UV region, indicating that the porphyrin macrocycle electronic structures have been modified. The changes in the UV–Vis spectra are very similar for both films, which could indicate that the same groups are oxidized. On the other hand, in case (2) similar changes in the absorption spectra were obtained during the oxidation processes (Fig. 6c and d). For the free base film, growing of two bands can be seen at 490 and 710 nm. For the Zn derivative the same band at 490 nm appears, and the broad band observed at 720 nm (Fig. 6b) is now shifted to 690 nm (Fig. 6d), and it is narrower compared with the one seen in case (1). Also upon oxidation PCBZTPA-Zn film presents the development of an absorption band in the near IR region (950 nm), and a bigger bleaching in the UV zone is observed for both films in the case (2).

It was mentioned above that both TPA and CBZ produce dimers when they are oxidized. Oxidation of TPB solutions have shown the apparition of a band at around 480 nm and a second broad band at about 680 nm at more anodic potential [49]. These two bands have been assigned to light absorption by radical cation and dication of TPB. Also related polymers containing TPB in their structures have shown similar absorption bands under oxidation, and a band at around 350 nm attributed to TPB in the reduced state [47,48]. On the other hand bands at 390 and

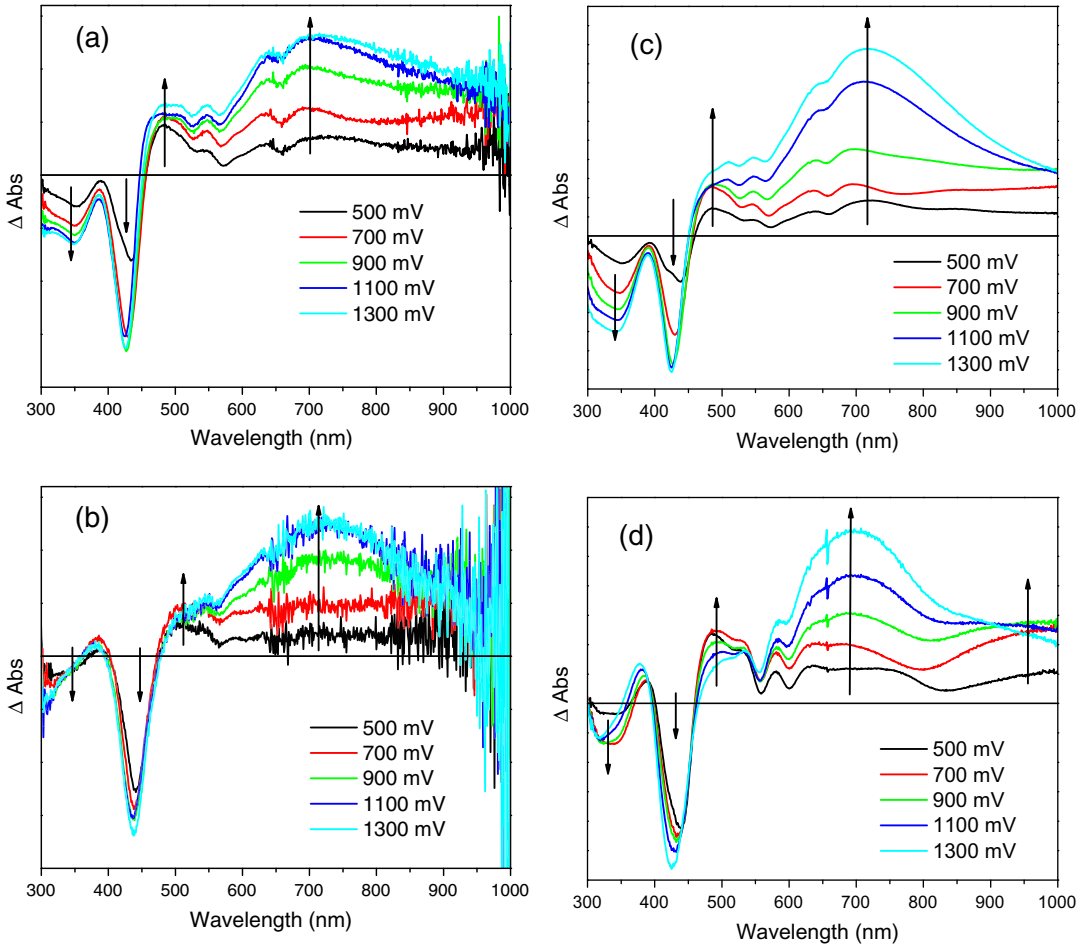

Fig. 6. Difference spectra of electropolymerized films of PCBZTPA (a) and PCBZTPA-Zn (b) in case (1), and of PCBZTPA (c) and PCBZTPA-Zn (d) in case (2) deposited on ITO, at different applied potentials in DCE solution with 0.1 M TBAPF6.

780 nm have been observed during electrolysis of dicarbazol, which were attributed to the absorption spectra of cation radical and dication of dicarbazol, respectively [41]. Oxidation of CBZ based polymers also depicted similar bands upon oxidation, and a band in the UV assigned to the DCBZ units before oxidation of the film [14,50,51]. Moreover, in a recent paper, we reported the electropolymerization of a meso substituted porphyrin by four *N*-ethyl carbazole groups. In the neutral state the film showed the typical porphyrin bands and a shoulder in the UV zone. Oxidation of the polymer presented a band that starts at 480–500 nm and it extends to IR. A second broad band was observed at more anodic potentials, with a maximum in the 600–750 nm range [12].

Based on the electrochemical and spectroelectrochemical studies, polymer structures in which the porphyrin units are linked by TPB and DCBZ groups are proposed (Fig. 1b). Oxidative polymerization does not happen when the peaks assigned to oxidation of porphyrins are cycled. Continuous cycling of any of the peaks corresponding to oxidation of TPA or CBZ produces an electroactive film on the electrode surface. Oxidation of the TPA or CBZ units in the monomers conducts to the formation of radical cations which react forming dimers, which are detected in the second cycle as a new redox couple. Posterior cycling of the monomers leads to the apparition of more radical cations which can produce more dimers or react with other dimers adsorbed in the electrode resulting in a longer chain. The difference in the polymerization efficiency in cases (1) and (2) may be due to a lower dimerization constant of TPA compared to the CBZ. The bigger bleaching in the UV zone in (2) is also in concordance with a lower dimerization constant. When the electrode is cycled in (1) just the TPA groups are dimerized, and the absorption in the UV zone is smaller than in (2). The bands at 485 nm and about 710 nm for free base film and 510 and 720 nm for Zn derivative observed during oxidation in case (1) could be assigned the radical cation and dication of TPB units. On the other hand the bands at 490 and 710 nm for PCBZTPA and 490 and 680 nm for PCBZTPA-Zn detected under oxidation in case (2) could be attributed to the radical cation and dication of DCBZ parts. The only difference between all the bands is for the PCBZTPA-Zn film grown cycling at applied potentials where oxidation of the CBZ units are produced. This film showed an absorption band in the IR, and the broad band was shifted to shorter wavelengths. These spectral changes are similar to those obtained during electropolymerization of a porphyrin substituted by four *N*-ethylcarbazol units [12].

Taking into account the above described results, it can be concluded that when the films are formed by cycling in the applied potential window where both functionalities are oxidized, linear polymers with some degree of cross-linkage are formed. This is due to the cross positions of the CBZ residues in the monomer structure and their bigger (4–5 orders of magnitude) radical cation coupling rate constants compared to those of the TPA groups.

The spectral changes observed upon redox switching between oxidized and reduced forms of the films produced different colorations. During these experiments we found strong and reversible electrochromic effects (Fig. 7) in ambient conditions. In the neutral state (0 V) the films are yellow pale, during the p-doping this color starts to change to greenish and finally, when the films are totally oxidized, a uniform green-bluish coloration is observed. As can be seen in the photographs, the electrogenerated colors are homogeneously distributed across the electrode surface, and the color changes are easily detected by the naked eye. This implies that the electro-deposited films have potential for electrochromic devices generation.

3.4. AFM images

The surface morphologies of the obtained polymer films were examined with AFM. Fig. 8a shows a typical Acoustic AC Mode AFM height mode image from the electrodeposited film of PCBZTPA on ITO. No difference in topological features was found for both PCBZTPA and PCBZTPA-Zn electropolymerized films. As it was previously reported for electrochemically generated porphyrin films, globular-like microstructures are observed in the analyzed films [7,20]. The observed microstructure must be a consequence of the nucleation and further growing process itself and not just a homogeneous decoration of the ITO surface (inset in Fig. 8a). This conclusion is confirmed by comparing the average surface RMS roughness measured over an area of 5 μm × 5 μm for the electrodeposited films, being 7.66 nm a much rougher surface than the ITO (1.32 nm).

In order to study the film thickness distribution on the electrode, we used AFM scratching, a technique which has been shown to be a suitable method for determination of the absolute thickness of the electrochemically deposited films [52]. Fig. 8b shows the profiles on different regions of the electrode covered by the PCBZTPA electrodeposited film. They clearly show the same thickness in the studied areas, the PCBZTPA-Zn electropolymerized films present the same behavior, concluding that the films grow with a homogeneous thickness distribution and without pinholes on the entire surface of the electrode. Also, the film thicknesses were determinated using a profiler, and the obtained values were correlated to the absorbance of the films. For both polymers it was observed that the thickness increases linearly with the absorbance. PCBZTPA showed that an increase in absorbance of 0.10 units at the Soret band corresponds to a ~19 nm change in the thickness, meanwhile PCBZTPA-Zn presented a change of ~10 nm for an increase of 0.1 units in the absorbance. The difference observed for the thicknesses of both polymers could be related to the higher molar extinction coefficient that present the Zn porphyrin derivatives compared to the free bases. The obtained thicknesses values by both techniques were very similar within the experimental error. It must be remarked that the films used for thickness determination were grown cycling the peak assigned to oxidation of CBZ units due to the cycling of the peak assigned to TPA conducted to the formation of very thin films.

3.5. Steady state and time resolved surface photovoltage spectroscopy

Fig. 9 shows the SPV (surface photovoltage) spectra of PCBZTPA and PCBZTPA-Zn electropolymerized on ITO.

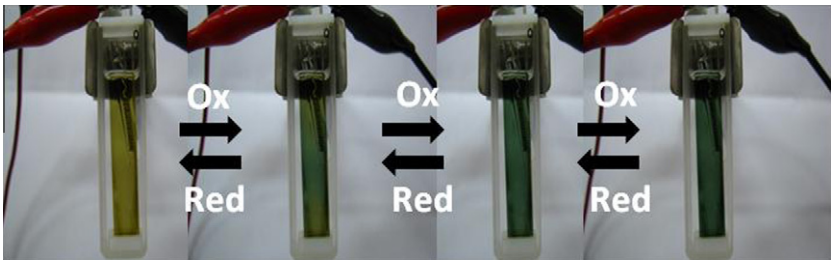

Fig. 7. Photograph images of PCBZTPA film deposited on ITO at various applied potentials.

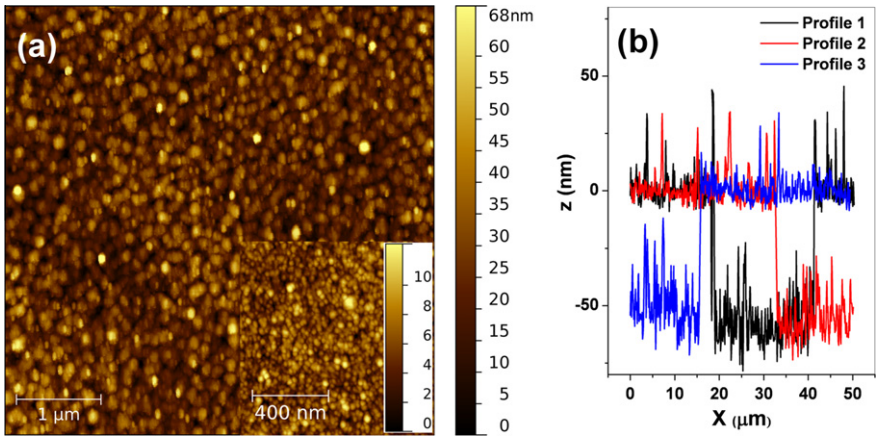

Fig. 8. (a) AFM images of ITO electrode surface (inset, scan size 1 × 1 μm) registered after electrodeposition of PCBZTPA films (scan size, 5 × 5 μm). (b) AFM section analysis used to evaluate the film thicknesses distributions on the electrode. Films were grown cycling the peak assigned to oxidation of the CBZ units.

The sign of the in-phase SPV signal is positive (negative) if the photo-generated electrons are preferentially separated towards the internal (external) surface. The absolute value of the in-phase signal is in maximum and the phase-shifted by 90° signal is zero, i.e. the phase angle is 0 or ±180°, if the time constants of the increasing and decreasing signals are much shorter than the modulation period. In contrast, the in-phase signal is zero and the absolute value of the phase-shifted by 90° signal is in maximum, i.e. the phase angle is ±90° or 270°, if the time constants of the increasing and decreasing signals are much longer than the modulation period. In this case, charge separation, transport processes and recombination are very slow, for example, limited by trapping with long trapping lifetimes. For PCBZTPA the sign of the in-phase SPV signal is positive, which denotes that the photogenerated electrons are separated towards the internal surface. Contrarily PCBZTPA-Zn shows a negative in-phase SPV signal indicating that the photogenerated electrons are separated towards the external surface.

Various peaks appeared in the SPV spectra. As remark, the electrode (quartz with SnO_2:F) strongly absorbed the light at photon energies above 3.6 eV. It will be interesting to compare SPV spectra directly with the absorption spectra. For this purpose information about the intensity dependence of the modulated SPV signals is needed. The amplitude of a modulated SPV signal is the square root of the sum of the squared in-phase and phase-shifted by 90° signals. As an example, the intensity dependence of the modulated PV amplitude measured at 600 nm is plotted in Fig. 10 for PCBZTPA-Zn in a double logarithmic scale. The SPV amplitude was proportional to the intensity of the illuminating light. This was a general behavior for both types of samples. It manifested additionally in the spectral dependence of the phase angle (cotan of the phase angle is defined as the ratio between the phase-shifted by 90° and in-phase signals) which was practically constant over the whole spectral range where SPV signals could be detected and which was independent of the intensity (see the insert of Fig. 10 for PCBZTPA-Zn). A constant phase angle means that the mechanisms of charge separation, transport and recombination are independent of the photon energy, i.e. excitations of the Q and Soret bands were equivalent with respect to charge separation and relaxation processes.

The SPV spectra could be normalized to the photon flux due to the facts that the PV amplitudes were proportional to the intensity and the separation and relaxation processes were independent of photon energy. The SPV spectra normalized to the photon flux are shown in Fig. 11 for PCBZTPA and PCBZTPA-Zn. For the free base polymer the SPV spectrum normalized to the photon flux presents bands at 433, 517, 568 and 654 nm and the SPV signal leveled out between 680 and 850 nm. The Zn derivative polymer shows bands at 441, 554, 597 nm and a broad shoulder at about 900 nm and leveling out at about

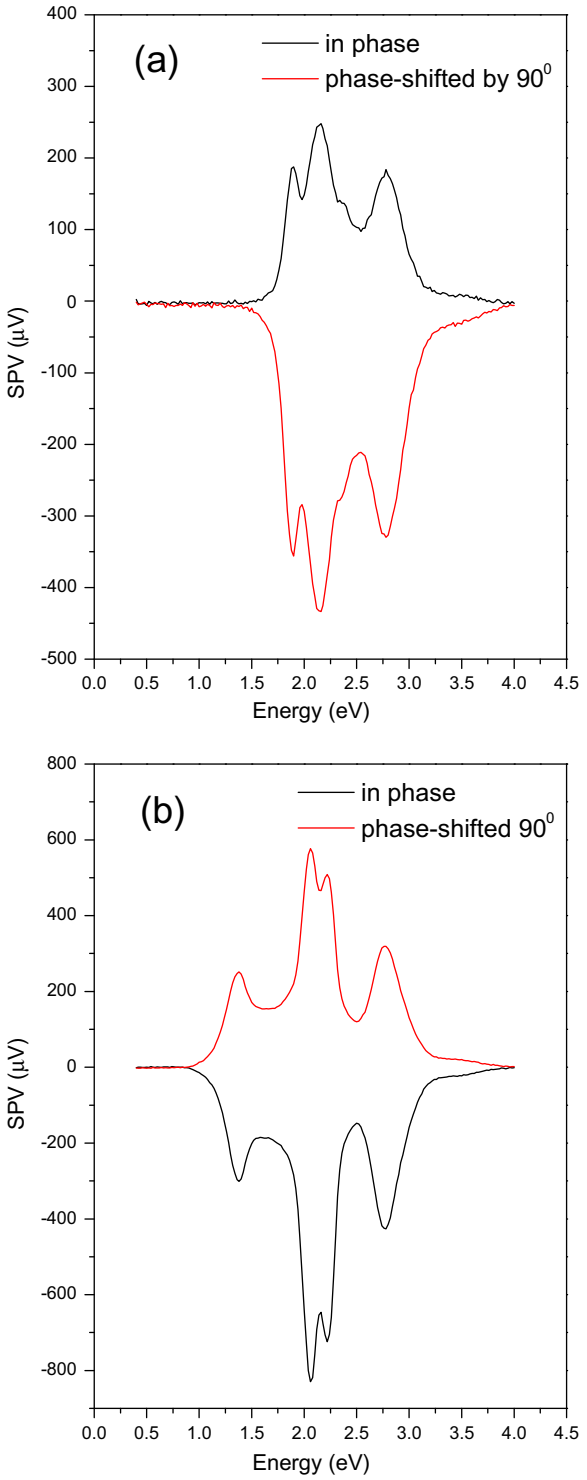

Fig. 9. Spectra of the in-phase and phase-shifted by 90° surface photovoltage signals for PCBZTPA (a) and PCBZTPA-Zn (b) electropolymerized on ITO.

1200 nm. In both films the bands in SPV spectra matched very well the absorption peaks of the polymers.

The directions of charge separation for both electropolymerized films on ITO were also confirmed by time

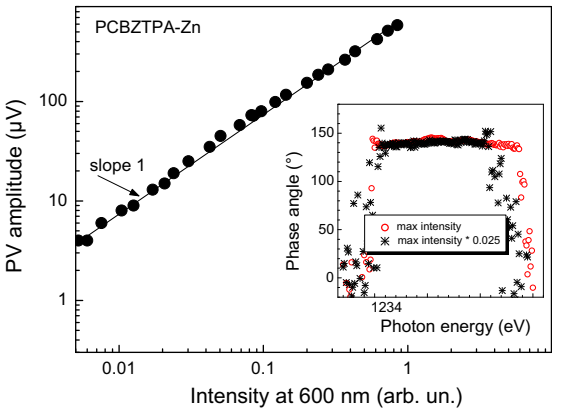

Fig. 10. Intensity dependence of the modulated SPV amplitude measured at 600 nm (PCBZTPA-Zn). The insert shows the spectra of the phase angle measured at maximum light intensity and decreased by 40 times using neutral filters.

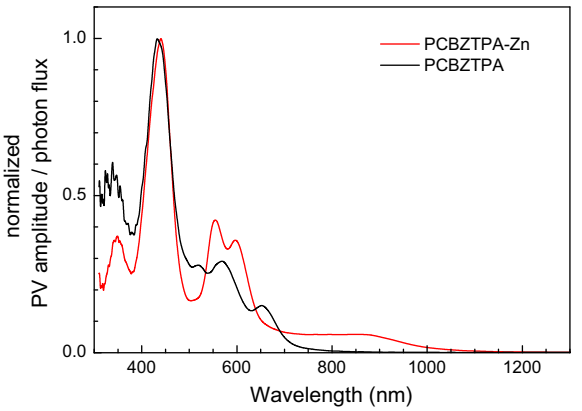

Fig. 11. Spectra of the SPV amplitude normalized to the photon flux for PCBZTPA (black line) and PCBZTPA-Zn (bold red line). (For interpretation of the references to color in this figure legend, the reader is referred to the web version of this article.)

resolved SPV measurements (Fig. 12), the electropolymers showed different signs in the SPV signals in concordance with the data obtained under chopped light illumination, i.e. positive for the free base and negative for the Zn(II) derivative. These experimental facts were observed for several studied samples of different absorbances and thus different thicknesses. In order to speculate about the type of charge separation and charge transport, more detailed knowledge about excitonic formation and transport, conductivity type, and band bending is necessary. These characterizations are under study, and the results will be reported in an incoming paper. It should be remarked that the transient SPV signals increased to about +40 mV and −40 mV within the laser pulse for PCBZTPA and PCBZTPA-Zn, respectively, and continued to increase within about 10^{-5} s by several mV for PCBZTPA (Fig. 12a) and −35 mV for PCBZTPA-Zn (Fig. 12b) at maximum light intensity while the period during which the SPV signals increased shifted to longer times with decreasing light intensity. The increasing SPV signals in time are an indication of

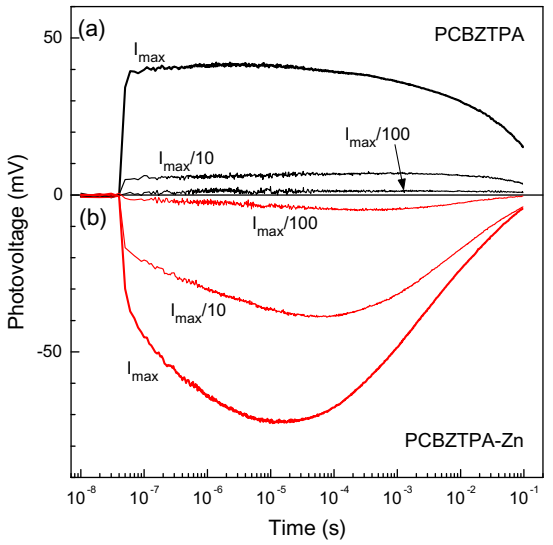

Fig. 12. Time resolved SPV signals for PCBZTPA (a) and PCBZTPA-Zn (b) electropolymerized on ITO measured at maximum intensity and at intensities decreased by 10 or 100 times.

ongoing charge separation by diffusion, i.e. preferential migration of one kind of photo-generated charge carriers. These findings show the high efficiency of both polymers in the generation of charge separation states, and that charge carriers are able to migrate making them promising candidates for application in optoelectronics devices.

4. Conclusions

Herein, we synthesized and characterized novel porphyrin derivatives with two different functionalities (TPA and CBZ) configured in a cross fashion. Due to the different radical cation coupling rate constants, linear polymers with some degree of cross-linkage are formed by electro-oxidation. Electro and spectroelectrochemical analysis allow proposing the formation mechanism of this stable and reproducible conducting polymeric structure holding porphyrin, a powerful optical and redox active center, tetraphenylbenzidine and dicarbazole, well-known hole-transporting materials. The spectral changes detected during redox processes of the films imply that the electro-deposited films have potential for electrochromic devices generation. Also, the films formed over semi-transparent surface showed the generation of photoinduced charge separation states and charge migration upon porphyrin excitation, making them promising candidates for application in optoelectronics devices.

Acknowledgments

Authors are grateful to Secretaría de Ciencia y Técnica, Universidad Nacional de Río Cuarto (Secyt-UNRC), Consejo Nacional de Investigaciones Científicas y Técnicas (CONICET) and Agencia Nacional de Promoción Científica y Tecnológica (ANPCYT) of Argentina for financial support. This work was supported by the Deutscher Akademischer Austausch Dienst (DAAD) – Ministerio de Ciencia, Tecnología e Innovación Productiva (MinCyT) join project (DA/10/06). M.G., F.F., E.N.D., G.M., and L.O., are Scientific Members of CONICET. J.D. and M.D.F. thank to CONICET, for research fellowships.

References

[1] B. Liu, W. Wu, X. Li, L. Li, S. Guo, X. Wei, W. Zhu, Q. Liu, Molecular engineering and theoretical investigation of organic sensitizers based on indoline dyes for quasi-solid state dye-sensitized solar cells, Phys. Chem. Chem. Phys. 13 (2011) 8985–8992.
[2] G. Heimel, I. Salzmann, S. Duhm, N. Koch, Design of organic semiconductors from molecular electrostatics, Chem. Mater. 23 (2011) 359–377.
[3] Y. Yang, F. Wudl, Organic electronics: from materials to devices, Adv. Mater. 21 (2009) 1401–1403.
[4] D. Gendron, M. Leclerc, New conjugated polymers for plastic solar cells, Energy Environ. Sci. 4 (2011) 1225–1237.
[5] A.L. Kanibolotsky, I.F. Perepichka, P.J. Skabara, Star-shaped π-conjugated oligomers and their applications in organic electronics and photonics, Chem. Soc. Rev. 39 (2010) 2695–2728.
[6] H.E. Katz, J. Huang, Thin-film organic electronic devices, Annu. Rev. Mater. Res. 39 (2009) 71–92.
[7] M. Gervaldo, M. Funes, J. Durantini, L. Fernandez, F. Fungo, L. Otero, Electrochemical polymerization of palladium(II) and free base 5,10,15,20-tetrakis(4-*N*,*N*-diphenylaminophenyl)porphyrins: its applications as electrochromic and photoelectric materials, Electrochim. Acta 55 (2010) 1948–1957.
[8] M. Li, S. Tang, F. Shen, M. Liu, W. Xie, H. Xia, L. Liu, L. Tian, Z. Xie, P. Lu, M. Hanif, D. Lu, G. Cheng, Y. Ma, Electrochemically deposited organic luminescent films: the effects of deposition parameters on morphologies and luminescent efficiency of films, J. Phys. Chem. B 110 (2006) 17784–17789.
[9] P.A. Liddell, M. Gervaldo, J.W. Bridgewater, A.E. Keirstead, S. Lin, T.A. Moore, A.L. Moore, D. Gust, Porphyrin-based hole conducting electropolymer, Chem. Mater. 20 (2008) 135–142.
[10] S. Tang, M. Liu, P. Lu, H. Xia, M. Li, Z. Xie, F. Shen, C. Gu, H. Wang, B. Yang, Y.G. Ma, A molecular glass for deep-blue organic light-emitting diodes comprising a 9,9′-spirobifluorene core and peripheral carbazole groups, Adv. Funct. Mater. 17 (2007) 2869–2877.
[11] M. Li, S. Tang, F. Shen, M. Liu, F. Li, P. Lu, D. Lu, M. Hanif, Y.J. Ma, The effects of supporting electrolytes on luminescent properties of electrochemical deposition films, Electrochem. Soc. 155 (2008) 287–291.
[12] J. Durantini, L. Otero, M. Funes, E.N. Durantini, F. Fungo, M. Gervaldo, Electrochemical oxidation-induced polymerization of 5,10,15,20-tetrakis[3-(*N*-ethylcarbazoyl)]porphyrin. Formation and characterization of a novel electroactive porphyrin thin film, Electrochim. Acta 56 (2011) 4126–4134.
[13] B. Lu, Y. Li, J. Xu, Electropolymerization study of benzothiophenes and characterization of novel poly(dibenzothiophene-S,S-dioxide), J. Electroanal. Chem. 643 (2010) 67–76.
[14] M. Lapkowski, J. Zak, K. Karon, B. Marciniec, W. Prukala, The mixed carbon–nitrogen conjugation in the carbazole based polymer; the electrochemical, UV–Vis, EPR, and IR studies on 1,4 bis[(E)2-(9H-carbazol-9-yl)vinyl]benzene, Electrochim. Acta 56 (2011) 4105–4116.
[15] K. Zhan, B. Tieke, J.C. Forgie, F. Vilela, J.A. Parkinson, P.J. Skabara, Cross-linked polymers based on 2,3,5,6-tetra-substituted pyrrolo[3,4-c]pyrrole-1,4(2H,5H)-dione (DPP): synthesis, optical and electronic properties, Polymer 51 (2010) 6107–6114.
[16] X. Huang, C. Zhu, S. Zhang, W. Li, Y. Guo, X. Zhan, Y. Liu, Z. Bo, Porphyrin-dithienothiophene π-conjugated copolymers: synthesis and their applications in field-effect transistors and solar cells, Macromolecules 41 (2008) 6895–6902.
[17] D. Wröbel, A. Siejak, P. Siejak, Photovoltaic and spectroscopic studies of selected halogenated porphyrins for their application in organic solar cells, Sol. Energy Mater. Sol. Cells 94 (2010) 492–500.
[18] T. Umeyama, T. Takamatsu, N. Tezuka, Y. Matano, Y. Araki, T. Wada, O. Yoshikawa, T. Sagawa, S. Yoshikawa, H. Imahori, Synthesis and photophysical and photovoltaic properties of porphyrin-furan and-thiophene alternating copolymers, J. Phys. Chem. C 113 (2009) 10798–10806.
[19] N. Xiang, Y. Liu, W. Zhou, H. Huang, X. Guo, Z. Tan, B. Zhao, P. Shen, S. Tan, Synthesis and characterization of porphyrin-terthiophene and oligothiophene π-conjugated copolymers for polymer solar cells, Eur. Polym. J. 46 (2010) 1084–1092.

[20] M.G. Walter, C.C. Wamser, Synthesis and characterization of electropolymerized nanostructured aminophenylporphyrin films, J. Phys. Chem. C 114 (2010) 7563–7574.
21] M.G. Walter, A.B. Rudine, C.C. Wamser, Porphyrins and phthalocyanines in solar photovoltaic cells, J. Porphyrins Phthalocyanines 14 (2010) 759–792.
[22] C.H.M. Maree, S.J. Roosendaal, T.J. Savenije, R.E.I. Schropp, T.J. Schaafsma, F.H.P.M. Habraken, Photovoltaic effects in porphyrin polymer films and heterojunctions, J. Appl. Phys. 80 (1996) 3381–3389.
[23] T. Akiyama, M. Matsushita, K. Kakutani, S. Yamada, K. Takechi, T. Shiga, T. Motohiro, H. Nakayama, K. Kohama, Solid-state solar cells consisting of polythiophene–porphyrin composite films, Jpn. J. Appl. Phys. Part 1 (44) (2005) 2799–2802.
[24] R. Charvet, S. Acharya, J.P. Hill, M. Akada, M. Liao, S. Seki, Y. Honsho, A. Saeki, K. Ariga, Block-copolymer-nanowires with nanosized domain segregation and high charge mobilities as stacked *p*/*n* heterojunction arrays for repeatable photocurrent switching, J. Am. Chem. Soc. 131 (2009) 18030–18031.
[25] J.Y. Lee, H.J. Song, S.M. Lee, J.H. Lee, D.K. Moon, Synthesis and investigation of photovoltaic properties for polymer semiconductors based on porphyrin compounds as light-harvesting units, Eur. Polym. J. 47 (2011) 1686–1693.
[26] H. Zhan, S. Lamare, A. Ng, T. Kenny, H. Guernon, W.-K. Chan, A.B. Djurisic, P.D. Harvey, W.-Y. Wong, Synthesis and photovoltaic properties of new metalloporphyrin-containing polyplatinyne polymers, Macromolecules 44 (2011) 5155–5167.
[27] M. Li, S. Ishihara, M. Akada, M. Liao, L. Sang, J.P. Hill, V. Krishnan, Y. Ma, K. Ariga, Electrochemical-coupling layer-by-layer (ECCLbL) assembly, J. Am. Chem. Soc. 133 (2011) 7348–7351.
[28] J.F. Ambrose, L.L. Carpenter, R.F. Nelson, Electrochemical and spectroscopic properties of cation radicals, J. Electrochem. Soc. Electrochem. Sci. Technol. 122 (1975) 876–894.
[29] J. Lia, A.C. Grimsdale, Carbazole-based polymers for organic photovoltaic devices, Chem. Soc. Rev. 39 (2010) 2399–2410.
[30] Z.-G. Zhang, Y.-L. Liu, Y. Yang, K. Hou, B. Peng, G. Zhao, M. Zhang, X. Guo, E.-T. Kang, Y.Y. Li, Alternating copolymers of carbazole and triphenylamine with conjugated side chain attaching acceptor groups: synthesis and photovoltaic application, Macromolecules 43 (2010) 9376–9383.
[31] C. Duan, K.-S. Chen, F. Huang, H.-L. Yip, S. Liu, J. Zhang, A.K.-Y. Jen, Y. Cao, Synthesis, characterization, and photovoltaic properties of carbazole-based two-dimensional conjugated polymers with donor-π-bridge-acceptor side chains, Chem. Mater. 22 (2010) 6444–6452.
[32] E. Wang, L. Hou, Z. Wang, Z. Ma, S. Hellström, W. Zhuang, F. Zhang, O. Inganäs, M.R. Andersson, Side-chain architectures of 2,7-carbazole and quinoxaline-based polymers for efficient polymer solar cells, Macromolecules 44 (2011) 2067–2073.
[33] L. Wang, Y. Fu, L. Zhu, G. Cui, F. Liang, L. Guo, X. Zhang, Z. Xie, Z. Su, Synthesis and photovoltaic properties of low-bandgap polymers based on *N*-arylcarbazole, Polymer 52 (2011) 1748–1754.
[34] Th. Dittrich, S. Bönisch, P. Zabel, S. Dube, High precision differential measurement of surface photovoltage transients on ultrathin CdS layers, Rev. Sci. Instrum. 79 (2008) 113903 (1-6).
[35] C.-W. Huang, K.Y. Chiu, S.-H. Cheng, Novel spectral and electrochemical characteristics of triphenylamine-bound zinc porphyrins and their intramolecular energy and electron transfer, Dalton Trans. 14 (2005) 2417–2422.
[36] I. Scalise, E.N. Durantini, Photodynamic effect of metallo 5-(4-carboxyphenyl)-10,15,20-tris(4-methylphenyl) porphyrins in biomimetic AOT reverse micelles containing urease, J. Photochem. Photobiol. A: Chem. 162 (2004) 105–113.
[37] J. Natera, L. Otero, L. Sereno, F. Fungo, N.-S. Wang, Y.-M. Tsai, T.-Y. Hwu, K.-T. Wong, A novel electrochromic polymer synthesized through electropolymerization of a new donor−acceptor bipolar system, Macromolecules 40 (2007) 4456–4463.
[38] D. Dolphin, The Porphyrins, Academic Press, London, 1978.
[39] K.M. Kadish, K.M. Smith, R. Guilard, The Porphyrin Handbook, Academic Press, San Diego, 2000.
[40] M. Gervaldo, F. Fungo, E.N. Durantini, J.J. Silber, L.E. Sereno, L. Otero, Carboxyphenyl metalloporphyrins as photosensitizers of semiconductor film electrodes. A study of the effect of different central metals, J. Phys. Chem. B 109 (2005) 20953–20962.
[41] J.F. Ambrose, R.F. Nelson, Anodic oxidation pathways of carbazoles, J. Electrochem. Soc. 115 (1968) 1159–1164.
[42] E.T. Seo, R.F. Nelson, J.M. Fritsch, L.S. Marcoux, D.W. Leedy, R.N. Adams, Anodic oxidation pathways of aromatic amines. Electrochemical and electron paramagnetic resonance studies, J. Am. Chem. Soc. 88 (1966) 3498–3503.
[43] R.F. Nelson, S.W. Feldberg, Chronoamperometric determination of the rate of dimerization of some substituted triphenylamine cation radicals, J. Phys. Chem. 73 (1969) 2623–2626.
[44] S.C. Creason, J. Wheeler, R.F. Nelson, Electrochemical and spectroscopic studies of cation radicals. Coupling rates of 4-substituted triphenylaminium ion, J. Org. Chem. 37 (1972) 4440–4446.
[45] G.A. Sotzing, J.L. Reddinger, A.R. Katritzky, J. Soloducho, R. Musgrave, J.R. Reynolds, Multiply colored electrochromic carbazole-based polymers, Chem. Mater. 9 (1997) 1578–1587.
[46] S. Koyuncu, B. Gultekin, C. Zafer, H. Bilgili, M. Can, S. Demic, I. Kaya, S. Icli, Electrochemical and optical properties of biphenyl bridged-dicarbazole oligomer films: electropolymerization and electrochromism, Electrochim. Acta 54 (2009) 5694–5702.
[47] L. Otero, L. Sereno, F. Fungo, Y.-L. Liao, C.-Y. Lin, K.-T. Wong, Synthesis and properties of a novel electrochromic polymer obtained from the electropolymerization of a 9,9′-spirobifluorene-bridged donor–acceptor (d–a) bichromophore system, Chem. Mater. 18 (2006) 3495–3502.
[48] C.L. Ramírez, A.R. Parise, Solvent resistant electrochromic polymer based on methylene-bridged arylamines, Org. Electron. 10 (2009) 747–752.
[49] M. Oyama, K. Nozaki, S. Okazaki, Pulse-electrolysis stopped-flow method for the electrospectroscopic analysis of short-lived intermediates generated in the electrooxidation of triphenylamine, Anal. Chem. 63 (1991) 1387–1392.
[50] S. Hayashida, K. Sukegawa, O. Niwa, Electrochemical oxidation of vacuum-deposited carbazole: preparation and film properties, Synth. Met. 35 (1990) 253–261.
[51] C. Chevrot, E. Ngbilo, K. Kham, S. Sadki, Optical and electronic properties of undoped and doped poly(*N*-alkylcarbazole) thin layers, Synth. Met. 81 (1996) 201–204.
[52] K. Bieńkowski, M. Strawski, M. Szklarczyk, The determination of the thickness of electrodeposited polymeric films by AFM and electrochemical techniques, J. Electroanal. Chem. 2011, doi:10.1016/j.jelechem.2011.06.014.